Chemistry & Biology, Vol. 10, 1115–1127, November, 2003, ©2003 Elsevier Science Ltd. All rights reserved. DOI 10.1016/j.chembiol.2003.11.001

Using Oxidative Crosslinking and Proximity Labeling to Quantitatively Characterize Protein-Protein and Protein-Peptide Complexes

Frank Amini, Carilee Denison, Hai-Jui Lin, Lillian Kuo, and Thomas Kodadek*
Center for Biomedical Inventions
Departments of Internal Medicine
and Molecular Biology
University of Texas Southwestern Medical Center
Dallas, Texas 75390

Summary

The quantitative analysis of protein-protein and protein-peptide complexes is of fundamental importance in biochemistry. We report here that nickel-catalyzed proximity biotinylation and Ru(II)(bpy)$_3^{2+}$-mediated oxidative crosslinking can be used to measure the equilibrium dissociation constant and stoichiometry of protein complexes. Only small amounts of protein are required, neither of the binding partners must be immobilized on a surface, and no special instrumentation is necessary. This chemistry should provide a useful complement to existing methods for the analysis of protein-protein and protein-peptide interactions.

Introduction

Protein-protein (or protein-peptide) interactions are important in most cellular processes [1, 2]. Of fundamental importance in the study of such interactions is to determine the affinity, kinetic half-life, and stoichiometry of a given complex, and many useful quantitative methods have been developed for this purpose. These include equilibrium sedimentation [3], fluorescence anisotropy [4], fluorescence resonance energy transfer (FRET) [5], coimmunoprecipitation and "pull-down" assays [6], surface plasmon resonance [7], and isothermal calorimetry [8, 9]. All of these methods have advantages and disadvantages. For instance, pull-down assays using glutathione-S-transferase (GST) fusion proteins are inexpensive and do not require large amounts of protein. However, they do require that one of the binding partners be immobilized on a solid surface. In some cases, the values measured in such a heterogeneous assay may not reflect the true solution values accurately due to avidity effects or other surface-related phenomena. Many of the methods employed to study protein-protein and protein-peptide interactions in solution require expensive equipment and/or large amounts of protein, including isothermal calorimetry, equilibrium sedimentation, and many others. More sensitive techniques, such as FRET, require the use of labeled proteins, and these modifications could likewise affect quantitative aspects of protein-protein interactions. Therefore, there is a continuing need to develop new quantitative methods to monitor protein-ligand interactions conveniently.

*Correspondence: thomas.kodadek@utsouthwestern.edu

Recently, we described two chemical methods that could have utility in this regard. The first is a proximity labeling technique (Figure 1A) that employs hexahistidine (His_6) or N-terminal glycine-glycine-histidine (NH_2-GGH)-tagged proteins. These tags bind Ni(II) tightly and, when oxidized with a peracid, a Ni(III) species is produced that is capable of mediating a variety of oxidative reactions, including DNA [10] and protein [11] cleavage and protein-protein crosslinking [12–15]. Brown and coworkers demonstrated that when the same oxidative reaction is carried out in the presence of high concentrations of biotin-tyramine, a radical reaction ensues that can result in the biotinylation of the nickel binding protein and other proteins in close proximity to it [16]. There are probably two general pathways that can lead to protein biotinylation (Figure 1A). In one, the peracid-activated nickel complex can abstract an electron from biotin-tyramine, resulting in the production of a diffusible radical that can couple to suitably reactive amino acids on the tagged protein or its neighbors (upper pathway, Figure 1). Alternatively, if the activated nickel complex is formed near an oxidizable protein side chain, such as a tyrosine or tryptophan, a protein-centered radical could be formed. This species could capture a biotin-tyramine from solution, again resulting in biotinylation (lower pathway, Figure 1A). However, if the radical is formed near the interface of the protein-protein complex, a covalent crosslink could result [13, 14]. This product could then be biotinylated in subsequent rounds of oxidation.

The second method is the oxidative crosslinking of proteins mediated by the tris(2,2′-bipyridyl)ruthenium(II) dication ((Ru(II)(bpy)$_3$)$^{2+}$), ammonium persulfate (APS), and visible light (Figure 1B). When Ru(II)(bpy)$_3^{2+}$, APS, and the proteins of interest are photolyzed briefly, efficient crosslinking of associated proteins is generally observed [17]. The reaction has been proposed to proceed through a Ru(III) intermediate formed by photoinitiated oxidation of the metal center by APS [18]. The Ru(III) complex can oxidize tyrosine or tryptophan side chains, creating a radical that can couple to appropriate nearby residues by a variety of pathways, some of which are shown in Figure 1B. Extensive studies of this reaction have demonstrated that only intimately associated proteins are crosslinked via this so-called "zero Å" chemistry. This protocol has now been utilized by several laboratories for the analysis of protein-protein interactions [19–25].

In this report, we show that these oxidative reactions can be used to measure the equilibrium dissociation constant (K_D) and stoichiometry of protein complexes. The reactions are simple to carry out, require no specialized equipment, and consume only small amounts of protein. We anticipate that this chemical methodology will provide a useful complement to instrument-based techniques for the quantitative study of protein-protein and protein-peptide interactions.

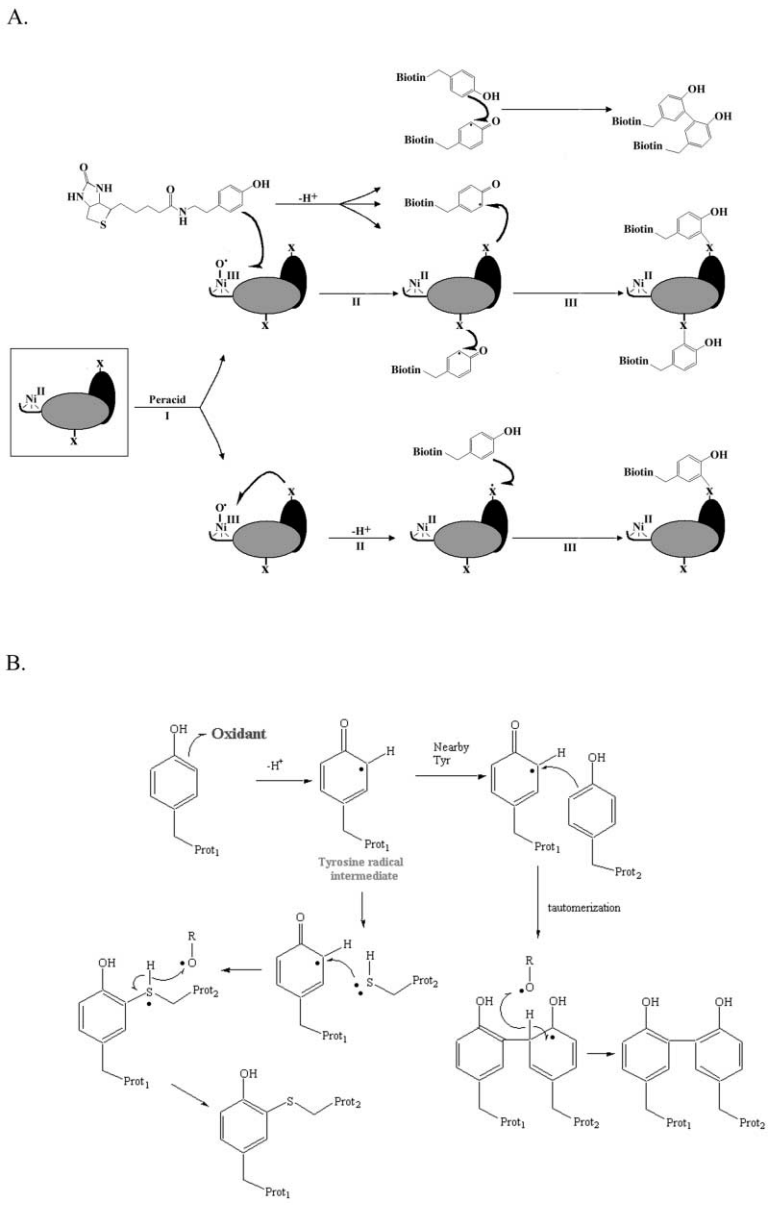

Figure 1. Proposed Mechanisms of Proximity Biotinylation and Oxidative Crosslinking

Results and Discussion

The Generation of N-Terminal GGH-Tagged Proteins for Proximity Labeling Reactions

NH_2-GGH binds Ni(II) extraordinarily tightly, with an estimated K_D of 10^{-16} M [26, 27]. Since few proteins are produced naturally with this tripeptide at the extreme N terminus, a general protocol was developed for the expression and purification of NH_2-GGH tagged proteins. A bacterial GST expression vector was constructed that encodes GGH upstream of the cloned gene and downstream of the residues encoding the TEV (tobacco etch virus) protease cleavage site. We call this vector pGEX-TEV-GGH (Figure 2A). A gene can be inserted into this vector and expressed in *E. coli*. Proteolytic cleavage would then free the NH_2-GGH protein from the resin (see Figure 2A).

To determine if NH_2-GGH-Ni(II)-mediated proximity labeling could be used for the quantitative analysis of protein-protein interactions, the complex of the yeast TATA binding protein (TBP) and a GST-Gal4 activation domain fusion protein (GST-AD) [28] was selected as the model system because it has been characterized previously. The TBP/GST-AD complex has a 1:2 stoichiometry and an equilibrium dissociation constant (K_D) of 200–300 nM [29]. Furthermore, both proteins are easily purified and are separable on a polyacrylamide gel. The yeast *TBP* open reading frame was subcloned into pGEX-TEV-GGH. The resultant construct, pGEX-TEV-GGH-TBP, was transformed into *E. coli* cells, expression was induced with IPTG, and the GST-TEV-GGH-TBP protein was purified from an extract by glutathione affinity chromatography. As shown in the Coomassie blue-stained polyacrylamide gel in Figure 2B, the affinity puri-

A.

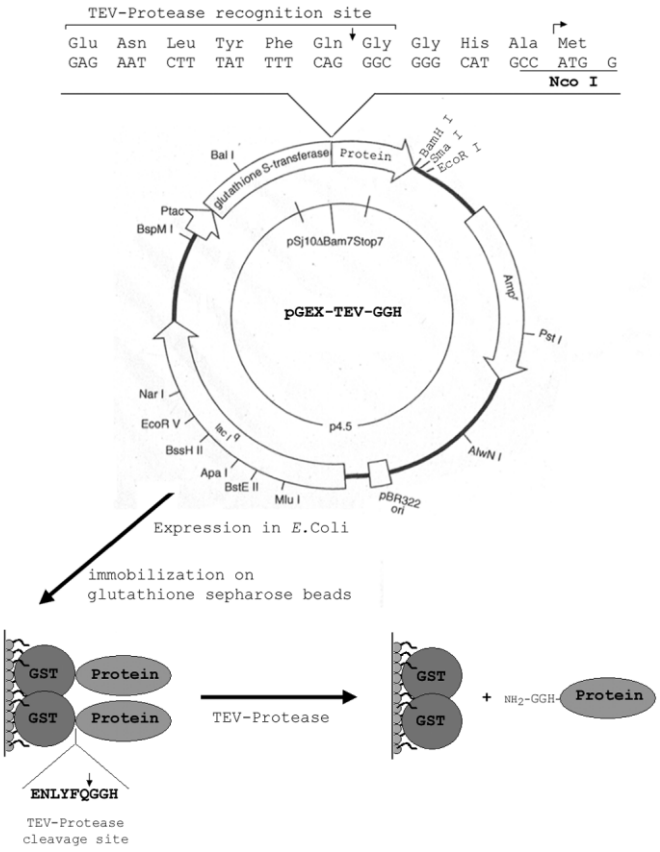

B.

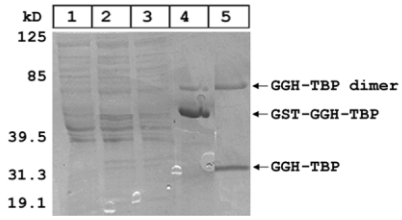

C.

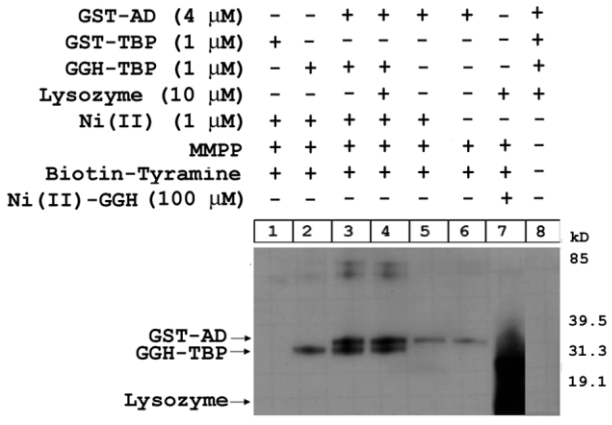

Figure 2. Proximity Labeling Reactions Using NH_2-GGH-TBP

(A) The map of pGEX-TEV-GGH and a purification scheme for the generation of GGH-tagged proteins.

(B) pGEX-TEV-GGH was used to express and purify GGH-TBP. A Coomassie blue-stained acrylamide gel is shown. Lane 1: extract from cells harboring pGEX-TEV-GGH. No induction. Lane 2: extract from cells harboring pGEX-TEV-GGH after induction with IPTG. Lane 3: cell extract after clearance with glutathione sepharose beads. Lane 4: boiled glutathione sepharose beads after incubation with the cell extract and several washing steps. Lane 5: the supernatant of the glutathione sepharose beads after treatment with TEV-protease.

(C) In the presence of an N-terminal GGH tag, Ni(II), MMPP, and biotin-tyramine, TBP mediates the localized proximity labeling of itself and its target protein. An HRP-avidin-probed blot is shown.

fied fraction contains a major protein with the mass expected of GST-TEV-GGH-TBP (lane 4). Upon TEV protease-mediated cleavage of immobilized GST-TEV-GGH-TBP, NH_2-GGH-TBP was released into the supernatant. As shown in lane 5, bands corresponding in molecular mass to the TBP monomer and dimer were detected. This was expected because the native TBP dimer is resistant to denaturation even under standard SDS-PAGE conditions [29–31]. We confirmed that the two major bands in lane 5 were indeed TBP by immunoblotting (data not shown). The presence of GGH at the N terminus of the protein was confirmed by Edman degradation (data not shown). These observations show that this approach is an effective means to produce N-terminal GGH-tagged proteins in pure form.

To probe the activity of this construct in a proximity labeling experiment, GGH-TBP was incubated with one equivalent of Ni(II)-acetate and then activated by MMPP in the presence of biotin-tyramine. The reactions were quenched and the products separated by SDS-PAGE. After transfer to a nitrocellulose membrane, the membrane was probed with a horseradish peroxidase-conjugated avidin (HRP-avidin) and developed with ECL (AP Biotech) in order to detect biotinylated products. As shown in Figure 2C, biotinylated GGH-TBP was detected (lane 2), whereas no labeling of the uncut GST-fusion protein was observed when it was incubated under the same conditions (lane 1). More importantly, GGH-TBP mediated the labeling of its binding partner, GST-AD, when it was included in the reaction (lane 3). However, the proximity labeling of lysozyme, a protein with which TBP does not associate, was not detected (lane 4). Lysozyme was labeled in the presence of exogenous Ni(II)-GGH (lane 7), showing that the result observed in lane 4 was not a trivial consequence of the lack of reactive residues on lysozyme. The affinity biotinylation reaction failed when Ni(II), the peracid MMPP, or biotin-tyramine were left out of the solution (data not shown). However, as shown in Figure 2C, lane 5, some GST-AD biotinylation was detected when the reaction was carried out in the absence of GGH-TBP. Biotinylation was still detected when Ni(II) was left out of the reaction (lane 6) but not when either MMPP or biotin-tyramine were excluded (data not shown). These observations show that some degree of "background" labeling can occur, presumably due to trace metals, but that this undesired reaction is significantly less efficient than the Ni/NH_2-GGH-mediated chemistry (lane 3). Taken together, the data show that the N-terminal GGH tag on TBP, in the presence of Ni(II), MMPP, and biotin-tyramine, specifically mediates the localized proximity labeling of TBP and its binding partner.

Measurement of the K_D of the GGH-TBP/GST-AD Complex by Proximity Labeling

Having validated the basic system qualitatively, we proceeded to ask if the K_D and stoichiometry of the complex could be determined by proximity labeling. For K_D measurements, 200 nM of NH_2-GGH-TBP was preincubated with an equimolar amount of Ni(II). Next, the Ni(II)-protein complex was incubated with 50 nM to 1 μM of GST-AD in separate tubes. Biotin-tyramine was then added, and the proximity labeling reaction was initiated by adding peracid to the samples. As a control for the nonspecific labeling of GST-AD, the reactions were repeated in the absence of GGH-TBP. The same volume of each sample was then loaded onto a tricine gel. After SDS-PAGE and transfer to a nitrocellulose membrane, the membrane was probed with alkaline phosphatase-conjugated streptavidin (APS-streptavidin). The membrane was then developed with an APS substrate (Figure 3A) and the chemiluminescence from each sample was measured with a STORM Imager (AP Biotech). For each sample, the chemiluminescence from proximity labeled GST-AD (lanes 2–7) was subtracted from its corresponding nonspecific chemiluminescence (Figure 3A, lanes 8–13). The derived values were then divided by the value from the sample with the highest GST-AD concentration (lane 7). This division yielded the relative labeling intensity of GST-AD at various concentrations (percent intensity), which was used to plot a saturation curve (Figure 3A, bottom left graph). A double reciprocal plot of these data indicated a K_D of 170 nM for the NH_2-GGH-TBP/$(GST\text{-}AD)_2$ complex (Figure 3A, bottom right graph). This value is very close to the 200 nM value derived using fluorescence polarization [29]. Therefore, proximity labeling can be used to measure the equilibrium dissociation constant of a protein complex.

Measurement of the Stoichiometry of the GGH-TBP/GST-AD Complex by Proximity Labeling

To determine if proximity labeling can be used to measure stoichiometry, 1 μM of Ni(II)-GGH-TBP, a concentration above the K_D of the complex, was titrated with 500 nM to 4 μM of GST-AD. The labeling reaction and analysis were then carried out as described previously. The saturation curve obtained showed that 2 μM GST-AD saturated 1 μM GGH-TBP, as expected (Figure 3B) [29], indicating that proximity labeling can be used to measure stoichiometry.

The Quantitative Characterization of the TBP/GST-AD Complex by His_6-Mediated Proximity Labeling

As mentioned previously, NH_2-GGH, because of its higher affinity for Ni(II), is the preferred tag for proximity labeling. However, His_6 does mediate this reaction [16]. It eliminates the requirement that the tag be on the extreme N terminus of the protein, and it is used much more commonly than NH_2-GGH. Therefore, we asked whether His_6-mediated proximity labeling could also be used as a quantitative tool.

The yeast *TBP* gene was subcloned into a bacterial expression vector in which the multiple cloning site was immediately downstream of a His_6-encoding sequence and a TEV-protease cleavage site [14]. In the presence of Ni(II), MMPP, and biotin-tyramine, His_6-TBP mediated the proximity labeling of itself and GST-AD (Figure 4A, lanes 2 and 3, respectively). The His_6 tag on TBP is required for proximity labeling, since very little biotinylation of TBP was detected when the tag was removed by TEV-protease-mediated proteolysis (Figure 4A, lane 1). Furthermore, His_6-mediated labeling is localized, since lysozyme was not labeled when it was included in the reaction (lane 4). Finally, Ni(II), MMPP, and biotin-tyramine were all required, since no biotinylation was

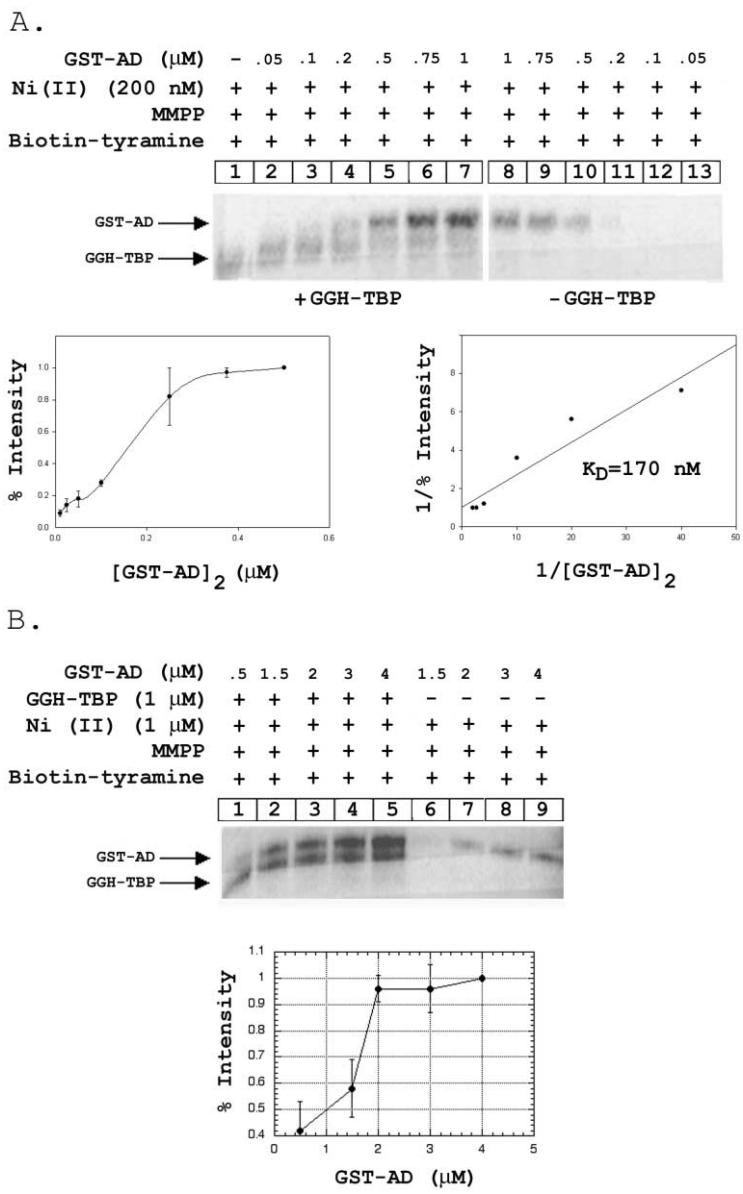

Figure 3. Using Proximity Labeling to Measure the K_D and Stoichiometry of the NH_2-GGH-TBP/GST-AD Complex

Proximity labeling was used to measure the K_D (A) and stoichiometry (B) of the GGH-TBP/GST-AD complex. APS-streptavidin-probed blots are shown. The graph was derived from data that had been background corrected. See text for details.

detected in the absence of each reagent (data not shown). The above observations indicate that the His_6 tag on TBP, like the GGH tag, is capable of mediating the localized proximity labeling of TBP and GST-AD.

We then asked whether the His_6 tag on TBP could be used to measure the K_D and stoichiometry of the His_6-TBP/$(GST\text{-}AD)_2$ complex, using the same methods employed for the NH_2-GGH-tagged protein. Based on the results, the His_6-TBP/GST-AD complex has a K_D of 240 nM (Figure 4B) and a 1:2 stoichiometry (Figure 4C). These measurements closely resemble both the published values [29] and those obtained by NH_2-GGH-mediated proximity labeling. Thus, the His_6 tag, like the GGH tag, can be used in proximity labeling experiments to characterize protein complexes quantitatively.

Quantitative Characterization of the GGH-RAD23/GST-Ubiquitin Complex by Proximity Labeling

Rad23 is a protein involved in yeast nucleotide excision repair. Recently, it has been observed that Rad23 forms a 1:1 complex with ubiquitin with a reported K_D of approximately 10 μM, as determined by a fluorescence-monitored solution titration experiment [32]. The K_D of the Rad23/ubiquitin complex was measured by proximity labeling in order to further test the methodology in the context of a modest affinity, labile complex.

Yeast *RAD 23* was subcloned into pGEX-TEV-GGH, and this expression vector was used to produce NH_2-GGH-Rad23 after TEV-mediated proteolysis. The *Saccharomyces cerevisiae* ubiquitin gene was subcloned into pGEX-TEV-GGH, expressed in *E. coli*, and the GST-ubiquitin (GST-Ub) fusion protein was purified by glutathione-affinity chromatography.

In the presence of Ni(II), biotin-tyramine, and MMPP, NH_2-GGH-Rad23 mediates its own biotinylation (Figure 5A, lane 3) and also labels GST-Ub (lane 4). The proximity biotinylation of uncut GST-Rad23 was not observed (data not shown). Little GST-Ub labeling was detected in the absence of NH_2-GGH-Rad23 (lane 6). As was the case for GST-AD, the low level of nonspecific labeling

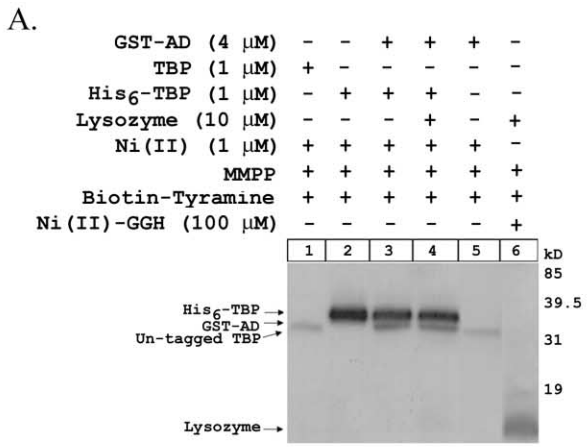

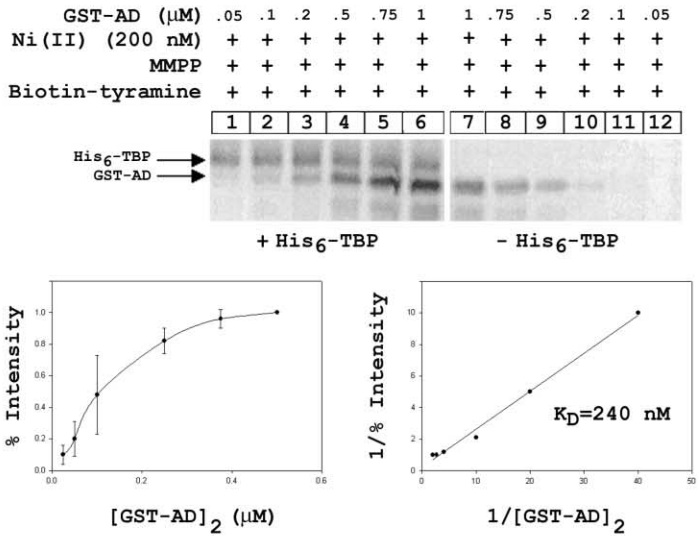

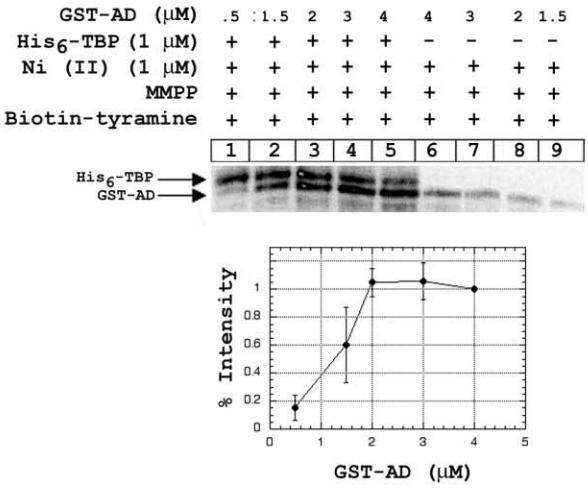

Figure 4. The Measurement of the K_D and Stoichiometry of the TBP/GST-AD Complex by His_6-Mediated Proximity Labeling

(A) The localized proximity labeling of GST-AD by His_6-TBP. In the presence of Ni(II), MMPP, and biotin-tyramine, the His_6 tag on TBP mediated the localized proximity labeling of TBP and GST-AD. Unlike NH_2-GGH-TBP, His_6-TBP migrates more slowly than GST-AD on an acrylamide gel. An HRP-avidin-probed blot is shown.

(B and C) The His_6 tag, like the GGH tag, can be used to measure the K_D (B) and stoichiometry (C) of the TBP/GST-AD complex. APS-streptavidin-probed blots are shown.

of GST-Ub did not require added Ni(II) (lane 7). Finally, labeling was localized, since lysozyme was not significantly labeled when it was included in the reaction (lane 5). Taken together, these data indicate that the NH_2-GGH tag on Rad23, like the GGH tag on TBP, supports the localized proximity labeling of itself and its binding partner.

To measure the K_D of this complex, 500 nM of NH_2-GGH-Rad23 was preincubated with an equimolar amount of Ni(II). Between 125 nM to 2 μM of GST-Ub was then added to the complex in separate tubes (Figure 5B, lanes 2–7). As controls for the nonspecific labeling of GST-Ub, samples without NH_2-GGH-Rad23 were also prepared (Figure 5B, lanes 8–13). The proximity labeling reaction was then carried out, and the samples were analyzed as described previously. Based on the obtained saturation curve (Figure 5B, bottom left graph) and double reciprocal plot (Figure 5B, bottom right graph), the NH_2-GGH-Rad23/GST-Ub complex has a K_D of 710 nM. This value is significantly lower than the published value, possibly due to the dimerization of ubiquitin by fusion to GST. Since Rad23 is known to be capable of dimerization [32], it is possible that some avidity effects may have contributed to this binding constant. Monomeric ubiquitin, which was used in the original study [32], was not used because GGH-Rad23 did not label the protein efficiently (data not shown). Ubiquitin was also not labeled by free NH_2-GGH/Ni(II) and MMPP, showing that this protein simply lacks appropriate residues on its surface to participate in this chemistry. Therefore, to better compare the proximity labeling result with an established method, the K_D of the protein complex was measured by a streptavidin-mediated pull-down assay. In brief, GGH-Rad23 was biotinylated with Biotin-NHS ester (Pierce) and immobilized on streptavidin M-280 Dynabeads (Dynal). Immobilized Rad23 was then incubated with 200 nM to 1 μM of GST-Ub. After several washes, the samples were boiled in loading buffer, loaded in entirety onto a gel, and separated by SDS-PAGE. After transfer to a nitrocellulose membrane, the membrane was probed with anti-GST antibody and an APS-conjugated secondary antibody. The membrane was then developed, and the relative intensity of GST-Ub in each sample was measured. A saturation curve and a double reciprocal plot were then obtained (Figure 5C), from which the K_D of the complex was measured to be 710 nM. The results confirm that proximity labeling can be used to measure the affinity of protein complexes.

It should be noted that K_D measurements are ideally performed under conditions in which most of the ligands are free. Hence, it would have been preferable to conduct the experiments in Figures 3–5 at much lower concentrations of GGH-tagged proteins. However, we have found that, at least for these particular systems, 300–600 ng of proteins per lane must be loaded onto the gel in order to detect biotinylated products, placing a limit on the lower limit of tagged protein that can be employed unless products are concentrated prior to analysis. The fact that these experiments were conducted at protein concentrations near the K_D of the complex, rather than well below it, probably explain the noticeable curvatures of the double reciprocal plots (Figures 3A and 5B, bottom left graphs). Whether or not this sensitivity limit will prove to be general remains to be determined and will require the analysis of many other protein complexes.

Proximity Labeling and Oxidative Crosslinking as Complementary Methods for the Analysis of Protein-Protein Interactions

Gal80 is a transcriptional repressor that binds tightly and specifically to the Gal4 AD [33–35]. The proximity labeling of the complex of the transcriptional repressor Gal80 with the Gal4 activation domain (Gal4-AD) was therefore also examined. As shown in Figure 6, His_6-Gal80 successfully mediated the proximity labeling of GST-AD (lane 2). A crosslinked, biotinylated product was also observed (lane 2).

Figure 6 also shows the results of an almost identical experiment in which the GST-AD construct was substituted with a different Gal4 derivative containing the DNA binding domain (DBD) and activation domain of the native protein (residues 1–93 and 768–881, respectively). We will refer to this protein as Gal4 DBD + AD. It was not biotinylated efficiently in a proximity labeling experiment (lane 4), suggesting that in the GST-AD experiment, labeling occurred on GST residues. When Gal4 DBD + AD was treated with Ni(II)-GGH and MMPP in *trans*, however, biotinylation of the protein was observed (lane 6). Taken together, these results indicate that while there are residues on Gal4 DBD + AD capable of coupling with a biotin-tyramine radical, they are either occluded in the Gal4 DBD + AD-Gal80 complex or are not close enough to the His_6 tag on Gal80 to be biotinylated.

The failure of the proximity labeling reaction is not particularly surprising, since no method can be expected to be completely general. This highlights the need for complementary methods. We therefore examined the ruthenium-mediated oxidative crosslinking process as a method for quantitative analysis. We note that studies by Teplow and coworkers of amyloid β protein-derived peptides [25, 36] and our own studies of the TBP-Gal4 AD complex [29] have been promising in this regard.

Figure 7A shows the results of experiments that employed a ^{32}P-labeled derivative of the Gal4 AD [14]. This was used in place of Gal4 DBD + AD because the latter is a stable dimer that can crosslink to itself as well as Gal80 (which is itself a dimer), leading to overly complex product distributions. The radiolabeled Gal4 AD protein (lane 1) is largely monomeric, and only low levels of crosslinking due to modest levels of aggregation of this polypeptide are observed in the absence of Gal80 (lane 2). The radiolabeled Gal4 AD was titrated with Gal80 to determine if photocrosslinking could be used to determine the stoichiometry of a protein complex. Thus, the concentration of the Gal4 AD was above the K_D of the complex, which is below 200 nM [37]. The stoichiometry of this complex is known to be 2:2 [17]. The solutions were photolyzed for one second immediately after the addition of $Ru(II)(bpy)_3^{2+}$ and ammonium persulfate (APS). Bands representing various Gal4 AD-Gal80 crosslinked products were evident in the autoradiogram of the SDS gel. The intensity of these bands increased until the Gal80 concentration was equivalent to that of the

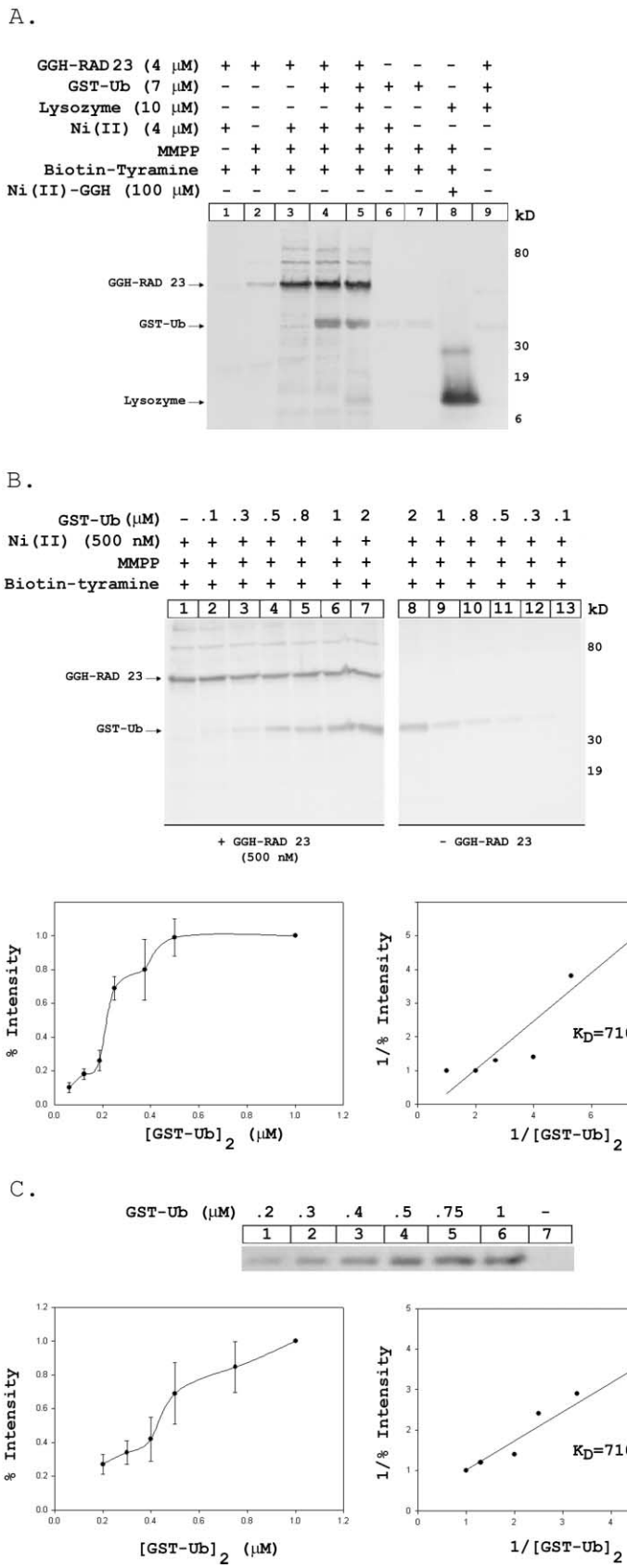

Figure 5. Measurement of the K_D of the NH_2-GGH-Rad23/GST-Ubiquitin Complex by Proximity Labeling

(A) NH_2-GGHRad23 mediates the localized proximity labeling of itself (lane 3) and its binding partner (lanes 4–5). An HRP-avidin-probed blot is shown.

(B) The measurement of the K_D of the NH_2-GGH-Rad23/GST-ubiquitin complex by proximity labeling. An APS-avidin-probed blot is shown.

(C) Measurement of the K_D of the NH_2-GGH-Rad23/GST-ubiquitin complex by the pull down of GST-Ub by biotinylated Rad23 on streptavidin beads. A membrane probed with anti-GST antibody and developed with an APS-conjugated secondary antibody is shown.

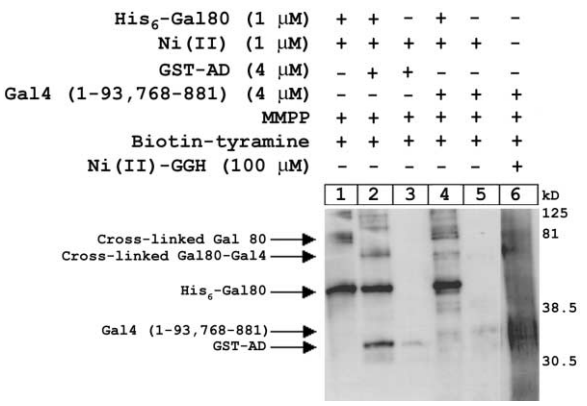

Figure 6. The Limits of Proximity Labeling

An HRP-avidin-probed blot is shown. His6-Gal80 mediated the proximity labeling of the Gal4 activation domain when it was fused to GST (GST-AD, lane 2) but not when it was fused to its DNA binding domain (Gal4-DBD + AD, lane 4). Gal4-DBD + AD was labeled when free Ni(II)-NH_2-GGH was added to the reaction in the absence of Gal80 (lane 6), indicating that the protein contains accessible residues for biotinylation in the unbound form.

Gal4 AD, consistent with the known stoichiometry (Figure 7A, lane 2 versus lanes 3–8). These observations show that Ru(II)$(bpy)_3^{2+}$-mediated photocrosslinking can be used to determine the stoichiometry of a protein complex.

Measurement of the K_D of a Protein-Peptide Complex by Ru(II)$(bpy)_3^{2+}$-Mediated Photocrosslinking

The association of proteins and small molecules or peptides is of fundamental importance in many areas of biology and pharmaceutical chemistry. In particular, synthetic ligands are increasingly being used to manipulate and analyze proteins [38–42]. Thus, it was of interest to ask if the photoinitiated crosslinking reaction could be employed to analyze these interactions quantitatively. As a model system, we employed Gal80 protein and a 20 residue Gal80 binding peptide that was isolated by phage display [37]. We are interested in Gal80 binding molecules as artificial activation domains for the construction of synthetic transcription factors [37, 43] and therefore would like to characterize in detail relevant protein interactions of this peptide.

Figure 7B shows the results of an experiment in which biotinylated Gal80 binding peptide (G80BP), present at a concentration (50 nM) below the K_D of the complex (300 nM) [37], was titrated with increasing concentrations of Gal80 protein in the presence of 0.2 mg/ml BSA to block nonspecific interactions. After crosslinking (or a mock control reaction in which the sample was not photolyzed), the solutions were analyzed by SDS-PAGE followed by probing with streptavidin to visualize the biotinylated species. In the absence of photolysis, no biotinylated proteins were observed, as expected (even-numbered lanes). In the crosslinked samples, increasing amounts of labeled protein were observed as the concentration of Gal80 protein increased. The most intense band corresponded to the expected molecular mass of Gal80, indicating crosslinking of the biotinylated peptide

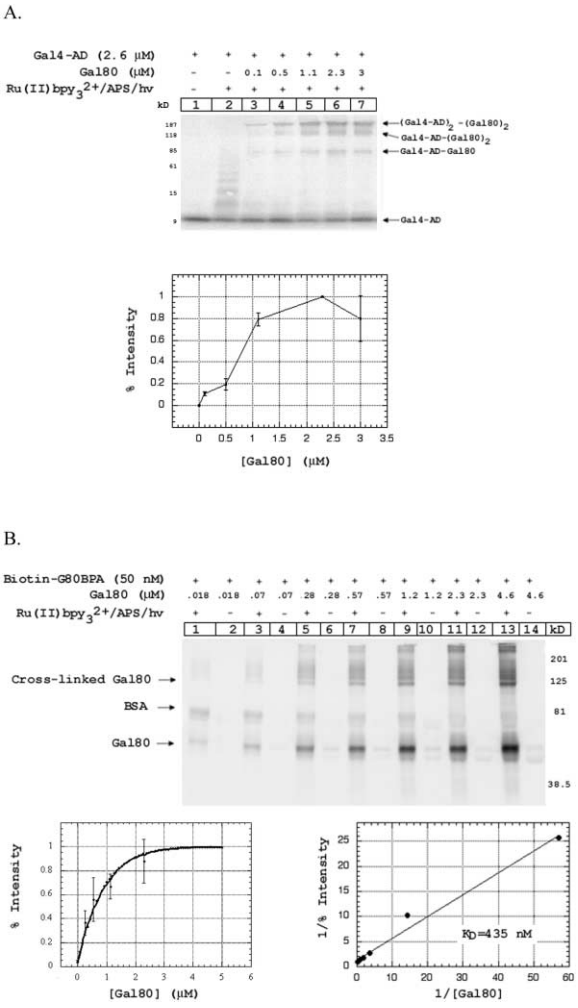

Figure 7. Measurement of the Stoichiometry and K_D of Protein Complexes by Photoactivated Crosslinking

(A) Measurement of the stoichiometry of the Gal4-AD/Gal80 complex by the quantification of the Ru(II)$(bpy)_3^{2+}$-mediated crosslinked Gal4 AD-Gal80 bands. An autoradiogram is shown.

(B) Measurement of the K_D of the G80BPA/Gal80 complex by photoactivated crosslinking. Ru(II)$(bpy)_3^{2+}$ was used to crosslink biotinylated G80BPA to increasing concentrations of Gal80. The crosslinked bands were quantified and used to measure the K_D (±10%) of the complex. An APS-streptavidin-probed blot is shown.

to a single molecule of Gal80. In addition, higher-order biotinylated products were present as well, resulting from a combination of crosslinking of biotinylated peptides and of Gal80 to itself (note that, at higher concentrations, Gal80 can tetramerize and further aggregate, resulting in products of high molecular mass) [17, 35]. When the intensity of the various products were plotted as a function of Gal80 concentration (bottom left of Figure 7B), a smooth titration curve was obtained. The double reciprocal plot indicated a K_D of 435 nM, similar to the value of 300 nM measured by fluorescence polarization with a fluorescein-tagged peptide [37].

Significance

The quantitative analysis of protein-ligand interactions is of fundamental importance in biochemistry. We have

shown that oxidative proximity labeling and crosslinking are convenient and complementary methods for this purpose. This chemistry allows proteins to be studied free in solution and only microgram quantities of substrate are required. We anticipate that these methods will complement existing techniques for the analysis of protein complexes and that they may be of particular utility with modest affinity complexes that are too labile kinetically to be studied using standard pull-down techniques.

Experimental Procedures

Plasmids

Construction of pGEX-TEV-GGH

PGEX-TEV-GGH was constructed as described previously [44]. In brief, the sequence encoding the TEV-Protease cleavage site of pGEX-cs [45] was removed by XhoI and NcoI double digestion. Next, the oligonucleotide 5′-TCGAGAATCTTTATTTTCAGGGCGG GCATGCCATGG-3′ was hybridized to the complementary oligonucleotide 5′-CATGGCATGCCCGCCCTGAAAATAAAGATTTCGAG-3′ (the sticky-end restriction sites of XhoI and NcoI are underlined). The resulting fragment, which encoded a GGH tripeptide downstream of a TEV-protease recognition site, was ligated into the digested pGEX-cs to generate pGEX-TEV-GGH (Figure 2A).

Construction of pGEX-TEV-GGH-TBP

Yeast *TBP* was amplified from the yeast genome by PCR via the primers 5′-CATGCCGCCATGGCCGATGAGGAA-3′ and 5′-CGCGG ATCCTCACATTTTTCTAAATTCAC-3′. The PCR fragment was then purified, double digested with NcoI and BamHI, and subcloned into pGEX-TEV-GGH.

Construction of pGEX-TEV-GGH-RAD 23

Yeast *RAD23* was amplified from the yeast genome by PCR via the primers 5′-CATGCCATGGTTAGCTTAACC-3′ and 5′-CGCGGATCC TCAGTCGGCATGATCGCTGAA-3′. The PCR fragment was then purified, double digested with NcoI and BamHI, and subcloned into pGEX-TEV-GGH.

Construction of His_6-HK_2-TEV-TBP

Yeast *TBP* was cleaved out of a pET-His_6-TBP expression vector [29] by digestion with NcoI and BamHI. The fragment was then purified by agarose gel extraction and subcloned into a His_6 expression vector that encoded two heart muscle kinase (HK_2) recognition sites immediately downstream of its tag [14]. This was done to slightly increase the molecular weight of His_6-TBP, which comigrated with GST-AD. For simplicity, His_6-HK_2-TBP was referred to as His_6-TBP.

Construction of pGEX-TEV-GGH-Ubiquitin

Yeast *Ubiquitin* was amplified from the plasmid pQE-31-His6-Myc-ubiquitin (C.D. and T.K., unpublished data) by PCR via the primers 5′-CATGCCATGGCCTATGAGCAAAAGC-3′ and 5′-CGCGGATCCT CACCCACCCCTC-3′. The PCR product was then double digested with NcoI and Bam HI, purified, and subcloned into pGEX-TEV-GGH. PGEX-TEV-GGH-ubiquitin contains the sequence for the peptide AMAYEQKLISEEDLPMHA between its GGH tag and ubiquitin (the myc tag is underlined).

Protein Purification

GST-Gal4 AD (comprising Gal4 residues 841–875) [28], His_6-Gal80 [37], and His_6-Gal4 (1–93, 768–881) [29, 46] were purified as described previously. The His_6 tag on Gal4 (1–93, 768–881) was cleaved by an overnight incubation with Factor Xa (Promega). His_6-P^{32}-Gal4-AD was purified and radiolabeled as described previously [14].

Purification of GGH-TBP

pGEX-TEV-GGH-TBP was transformed into BL21-DE3-RIL cells (Invitrogen). A colony was grown overnight at 37°C in 300 ml of LB containing 50 μg/ml of Ampicillin (LB-Amp). The culture was then transferred to six flasks with 1 liter of LB-Amp in each. The cells were induced with 100 μM of isopropyl-1-thio-β-D-galactopyranoside (IPTG) once the optical density at 595 nm (OD_{595}) reached 0.4–0.6. After 3 hr of growth following induction, the cells were harvested, washed with 200 ml of 1X-PBS, and resuspended in 100 ml of sonication buffer (1X-PBS, 0.1% Tween-20, 1 mM PMSF, Roche protease inhibitor tables). The suspension was then sonicated six times at 300 watts in bursts of 10 s. Each sonication event was followed by 2 min of incubation on ice. The lysate was spun down at 22,000 rpm, and the supernatant was loaded onto a column packed with 5 ml of Amersham Glutathione-Sepharose 4-B beads preequilibriated with 10 ml of sonication buffer. Next, the column was washed with 1X-PBS + 0.1% Tween 20 until no protein was detected from the flowthrough by Bradford's Assay. The beads were then washed once with 50 ml of 1X-PBS + 15% glycerol and suspended in 3 ml of the same buffer. TEV protease (40 μl; Invitrogen) was added, and the mixture was rotated at 4°C for 16–18 hr. The beads were then repacked onto a column and the flowthrough was collected and concentrated to 1 ml. The protein prep was dialyzed into 1X-PBS + 15% glycerol three times to get rid of the EDTA in the TEV protease storage buffer (EDTA is a potent inhibitor of proximity labeling). Finally, the presence of GGH at the N terminus of TBP was confirmed by Edman degradation. The protein was stored at −80°C in aliquots.

Purification of GGH-RAD 23

The same methodology used to purify GGH-TBP was used to purify GGH-Rad23.

Purification of His_6-TBP

The His_6-TBP expression vector was transformed into BL21-DE3-RIL cells, grown overnight at 37°C in LB-ampicillin, and transferred to six flasks with 1 L of LB-ampicillin in each. The cells were grown at 37°C until an OD_{595} of 0.5 was reached. At that point, the cells were induced with 1 mM of IPTG and grown for another 4 hr at the same temperature. The cells were then harvested and washed as described previously. Next, the cells were resuspended in 100 ml of sonication buffer (300 mM NaCl, 50 mM $NaHPo_4$, 0.1% Tween-20, Roche protease inhibitor tablets [pH 8]). The suspension was then sonicated and spun down as previously described. The supernatant was loaded onto a column packed with 5 ml of Ni-NTA beads preequilibriated with 10 ml of sonication buffer. Next, the column was washed with wash buffer (500 mM NaCl, 50 mM $NaHPo_4$, 0.1% Tween-20, 25 mM imidazole [pH 8]) until no protein was detected from the flowthrough. Finally, His_6-TBP was eluted from the column by elution with wash buffer that contained 500 mM imidazole. Fractions containing TBP were pooled, buffer exchanged into 1X-PBS + 15% glycerol using a PD-10 column (Amersham), and stored at −80°C in aliquots.

Purification of GST-Ubiquitin

PGEX-TEV-GGH-ubiquitin was transformed into BL21-DE3-RIL cells (Invitrogen). The cells were grown, induced, harvested, and sonicated by the same protocol that was used for GGH-TBP purification. After sonication, the extract was spun down, immobilized on glutathione beads, and washed as described previously. Subsequently, the beads were resuspended in 3 ml of 1X-PBS + 15% glycerol + 10 mM glutathione. After 10 min of rotation at 4°C, the beads were repacked onto a column. The flowthrough was collected and concentrated to 1 ml. In order to get rid of excess glutathione, the protein prep was then dialyzed into 1X-PBS + 15% glycerol three times (like EDTA, glutathione inhibits proximity labeling). Finally, the protein was collected and stored at −80°C in aliquots.

Proximity Labeling Reactions

In all the proximity labeling reactions, an equimolar amount of Ni(II) acetate tetrahydrate ($Ni(OAc)_2$) was preincubated with the NH_2-GGH- or His_6-tagged protein for 15 min at room temperature. The target protein was then added, and the samples were incubated at room temperature for 5–15 more minutes. Lysozyme was then added to some samples, and all the samples were incubated for 5 more minutes at room temperature. Subsequently, the samples were diluted in crosslinking buffer (150 mM NaCl, 150 mM $NaPO_4$ [pH 7]) and biotin-tyramine [16] was added. Freshly prepared magnesium monoperoxy-phthalate hexahydrate (MMPP) was then added. After incubating for 2 min at room temperature, the samples were quenched with loading buffer (0.24 M Tris, 8% SDS, 2.88 M β-Mercaptoethanol, 40% glycerol, and 0.4% bromophenol blue) and boiled at 100°C for 5 min. Before quenching, the final concentrations of biotin-tyramine, MMPP, and lysozyme in all the reactions were 250 μM, 500 μM, and 10 μM, respectively. In some samples, preincu-

bated Ni(II)-GGH complexes were added to final (prequenched) concentrations of 100 μM. The final volumes of the proximity labeling reactions were 15 μl, 30 μl, or 60 μl. These reactions were quenched with 5 μl, 10 μl, or 20 μl of loading buffer, respectively.

Proximity Labeling of the TBP/GST-AD Complex

NH_2-GGH-TBP or His_6-TBP was preincubated with Ni(II). GST-AD was then added to some samples followed by 5 min of incubation. Lysozyme was then added to some samples. Next, the samples were diluted in crosslinking buffer, biotin-tyramine was added, and the reactions were initiated by the addition of MMPP. Before quenching, the final concentrations of GGH-TBP, His_6-TBP, and Ni(II) were 200 nM. The final volume of the reactions before quenching was 15 μl. After quenching, 5 μl of each sample was loaded onto a Tricine-SDS polyacrylamide gel [47] and separated by electrophoresis. A 10% Tricine gel was used to separate GGH-TBP from GST-AD, while a 15% gel was used to separate His_6-TBP from GST-AD. The gels were then transferred onto a nitrocellulose membrane, probed with avidin-HRP (Pierce, 5 μg/ml), and visualized by chemiluminescence (Pierce, SuperSignal West Pico Chemiluminescent Substrate).

Measurement of the K_D of the TBP/GST-AD Complex

Ni(II)-NH_2-GGH-TBP or Ni(II)-His_6-TBP complexes were incubated with various concentrations of GST-AD for 5 min. Proximity biotinylation reactions were then initiated as described previously. The final volume of the reactions was 60 μl before quenching. The final concentrations of GGH-TBP, His_6-TBP, and Ni(II) were 200 nM. The samples were loaded in entirety onto a Tricine-SDS polyacrylamide gel and separated by electrophoresis. After transfer to a nitrocellulose membrane, the membrane was probed with alkaline phosphatase (APS)-conjugated streptavidin (Molecular Probes, 4 μg/ml) and developed with Amersham's AttoPhos signal amplification reagent. The chemiluminescence from each reaction was then measured by Amersham's STORM fluorimager. The specific labeling volume of GST-AD by His_6-TBP or GGH-TBP was measured by subtracting the proximity labeled GST-AD volume from the nonspecifically labeled volume [i.e., the labeling of GST-AD by Ni(II), MMPP, and biotin-tyramine alone]. The percent intensity of GST-AD at each concentration was then calculated by dividing the specific labeling volume of GST-AD at that concentration by the specific labeling volume of the highest GST-AD concentration in the experiment. Finally, the percent intensities of GST-AD at various concentrations were calculated and plotted as percent intensity versus $[(GST\text{-}AD)]_2$ with the program Kaleidograph. GST-AD concentrations were divided by two because the protein is a dimer. The double reciprocal plot of percent intensity versus $[GST\text{-}AD]_2$ was then plotted, from which a best-fit line was obtained. The slope of the line was considered to be the K_D of the TBP/GST-AD complex.

Measurement of the Stoichiometry of the TBP/GST-AD Complex

Various concentrations of GST-AD were added to tubes containing preincubated Ni(II)-GGH-TBP or Ni(II)-His_6-TBP complexes. After 5 min of incubation, the samples were diluted in crosslinking buffer, and biotin-tyramine was added. The proximity biotinylation reactions were then carried out as described previously. Before quenching, the final concentrations of the tagged protein and Ni(II) were 1 μM. The final reaction volume before was 15 μl. The quenched samples (5 μl) were loaded onto a gel and separated by SDS-PAGE. The gel was transferred onto a nitrocellulose membrane, probed with APS-streptavidin, developed, and analyzed as described previously. The percent intensity of GST-AD at each concentration was then calculated and plotted as percent intensity versus GST-AD.

Proximity Labeling of the His_6-Gal80/Gal4-AD Complex

His_6-Gal80 was incubated with Ni(II) for 15 min at room temperature. GST-AD or Gal4-AD was then added to some samples. After 5 min of incubation, the samples were diluted in crosslinking buffer, biotin-tyramine was added, and the reaction was initiated by MMPP addition. After quenching, 5 μl of each sample was loaded onto a gel and separated by SDS-PAGE. The gels were then transferred onto a nitrocellulose membrane, probed with avidin-HRP, and visualized by chemiluminescence. Final concentrations of Ni(II)-His_6-Gal80 and the Gal4 derivatives were 1 μM and 4 μM, respectively. The final volume of the reactions before quenching was 15 μl.

Proximity Labeling of the GGH-Rad23/GST-Ubiquitin Complex

GGH-RAD 23 was incubated with Ni(II) for 15 min at room temperature. GST-ubiquitin was then added to some samples followed by 15 more min of incubation. Lysozyme was added to some samples at this time, and the samples were incubated for another 5 min. The samples were then diluted in crosslinking buffer, biotin-tyramine was added, and the reactions were initiated as described previously. After quenching, 10 μl of each sample was loaded onto a gel for SDS-PAGE. The gel was then transferred to a membrane and probed with HRP-avidin. Final concentrations of Ni(II)-GGH-Rad23 and GST-ubiquitin were 4 μM and 7 μM, respectively. The final volume of the reactions before quenching was 15 μl.

Measurement of the K_D of the GGH-Rad23/GST-Ubiquitin Complex by Proximity Labeling

Various concentrations of GST-ubiquitin were added to preincubated Ni(II)-GGH-RAD 23 complexes, and the resulting solution was incubated for 15 min. The samples were then diluted, biotin-tyramine was added, and the proximity biotinylation reactions were initiated. After quenching, the samples were loaded in entirety onto a tricine gel and analyzed as described previously. The final concentration of the Ni(II)-GGH-RAD 23 complex was 500 nM, and the final volume of the reactions before quenching was 30 μl.

Measurement of the K_D of the Rad23/GST-Ub Complex by Streptavidin Pull-Down Assays

About 2.5 mg of streptavidin M-280 Dynabeads (Dynal, Inc.) were washed twice in crosslinking buffer and incubated with 1 ml of bacterial extract (15 μg/μl in crosslinking buffer) at room temperature for 30 min. The beads (900 μl) were then incubated with biotinylated Rad23 (10 μg) at room temperature for 15 more minutes. Next, the beads were washed three times with 1 ml of wash buffer (100 mM HEPES, 200 mM potassium acetate, 10 mM magnesium acetate, 2 mM EDTA, 20% glycerol, and 1% Tween-20 [pH 7.5]) and resuspended in 1 ml of bacterial extract. Tubes with 50 μl of beads were then prepared and incubated with 1 μl of GST-Ub at various concentrations at room temperature for 15 min. As a control for the nonspecific binding of GST-Ub to streptavidin beads, 1 μM of GST-Ub was incubated with 50 μl of streptavidin beads without Rad23 (Figure 5C, lane 7). After incubation, the beads were washed four times in wash buffer and resuspended in 30 μl of loading buffer. The beads were then boiled for 5 min, and the supernatants of each sample were loaded in entirety onto a gel. After separation by SDS-PAGE, the samples were transferred to a nitrocellulose membrane and probed with mouse-anti-GST antibody (Santa Cruz Biotechnology). The membrane was then probed with APS conjugated goat-anti-mouse secondary antibody (Biorad), developed, and analyzed as described previously. GGH-Rad23 was biotinylated with Biotin-NHS (Pierce) as described in Pierce product description handout #21430.

Synthesis of Biotinylated G80BPA

Gal80 binding peptide A (G80BPA) [37] was synthesized on a Symphony peptide synthesizer (Protein Technologies) and purified by HPLC. For detection purposes, a linker region of two glycines and a biotinylated lysine residue were attached to the N terminus of the original G80BP-A sequence. Hence, the full-length sequence of biotinylated G80BP-A was NH_2-K(B)GGYDQDMQNNTFDDLFWKE GHR-COOH.

The Measurement of the K_D of the Gal80/G80-BPA Complex

Different concentrations of His_6-Gal80 were mixed with 50 nM of G80BPA. The volumes of the samples were then raised to 30 μl with 1X-PBS containing 0.2 mg/ml bovine serum albumin. Next, the mixtures were incubated at room temperature and tumbled for 30 min. The samples were then photocrosslinked as described previously [17, 18]. In brief, $Ru(bpy)_3^{2+}$ and APS were added to the samples to final concentrations of 125 μM and 2.5mM, respectively.

Immediately thereafter, the samples were exposed to visible light for 1 s. The irradiated samples were then quenched with 30 μl of loading buffer. Control samples that contained no $Ru(bpy)_3^{2+}$ or APS and were not exposed to visible light were also prepared. Both the crosslinked and control samples were denatured at 95°C for 5 min, separated by SDS-PAGE, and transferred onto a nitrocellulose membrane. The biotinylated crosslinked products were blotted with APS-streptavidin and visualized with the AttoPhos fluorescent substrate. The blue fluorescence signals derived from the crosslinked products were then detected and analyzed as described previously.

Stoichiometry Determination of the Gal4-Gal80 Complex

Reactions containing 2.6 μM radiolabeled His_6-P^{32}-Gal4-AD and varying concentrations of Gal80 (0, 0.1, 0.5, 1.1, 2.3, and 3 μM) were incubated on ice for 30 min. The solutions were then photolyzed for 1 s in the presence of 125 μM $Ru(bpy)_3^{2+}$ and 2.5 mM ammonium persulfate. Samples were quenched with loading buffer and separated on a 9% denaturing polyacrylamide gel. The gel was dried down and exposed to a phosphoimager cassette overnight. Results were visualized on the STORM phosphoimager and quantitated with Image-Quant software. All of the results shown are the result of three independent experiments.

Supplemental Data

Two Supplemental Figures for this manuscript are available online at http://www.chembiol.com/cgi/content/full/10/11/1115/DC1.

Acknowledgments

This work was supported by grants from the National Institutes of Health (GM 58175) and the Welch Foundation (I-1299).

Received: May 22, 2003
Revised: September 4, 2003
Accepted: September 8, 2003
Published: November 21, 2003

References

1. Alberts, B. (1998). The cell as a collection of protein machines: preparing the next generation of molecular biologists. Cell *92*, 291–294.
2. Alberts, B.M. (1984). The enzymology of DNA protein machines. Cold Spring Harb. Symp. Quant. Biol. *49*, 1–12.
3. Minton, A.P. (2000). Quantitative characterization of reversible macromolecular associations via sedimentation equilibrium: an introduction. Exp. Mol. Med. *32*, 1–5.
4. Heyduk, T., Ma, Y., Tang, H., and Ebright, R.H. (1996). Fluorescence anisotropy: rapid, quantitative assay for protein-DNA and protein-protein interactions. Methods Enzymol. *274*, 492–503.
5. Mitra, R.D., Silva, C.M., and Youvan, D.C. (1996). Fluorescence resonance energy transfer between blue-emitting and red-shifted excitation derivatives of the green fluorescent protein. Gene *173*, 13–17.
6. Phizicky, E.M., and Fields, S. (1995). Protein-protein interactions: methods for detection and analysis. Microbiol. Rev. *59*, 94–123.
7. Rich, R.L., and Myszka, D.G. (2000). Advances in surface plasmon resonance biosensor analysis. Curr. Opin. Biotechnol. *11*, 54–61.
8. Ladbury, J.E., and Chowdhry, B.Z. (1996). Sensing the heat: the application of isothermal titration calorimetry to thermodynamic studies of biomolecular interactions. Chem. Biol. *3*, 791–801.
9. Leavitt, S., and Freire, E. (2001). Direct measurement of protein binding energetics by isothermal titration calorimetry. Curr. Opin. Struct. Biol. *11*, 560–566.
10. Mack, D.P., and Dervan, P.B. (1992). Sequence-specific oxidative cleavage of DNA by a designed metalloprotein, Ni(II)GGH (Hin139–190). Biochemistry *31*, 9399–9405.
11. Cuenoud, B., Tarasow, T.M., and Schepartz, A. (1992). A new strategy for directed protein cleavage. Tetrahedon Lett. *33*, 895–898.
12. Brown, K.C., Yang, S.-H., and Kodadek, T. (1995). Highly specific oxidative crosslinking of proteins mediated by a nickel-peptide complex. Biochemistry *34*, 4733–4739.
13. Fancy, D., Melcher, K., Johnston, S.A., and Kodadek, T. (1996). New chemistry for the study of multiprotein complexes: the six histidine tag as a receptor for a protein crosslinking reagent. Chem. Biol. *3*, 551–559.
14. Fancy, D., and Kodadek, T. (1997). Site-directed oxidative protein crosslinking. Tetrahedron *53*, 11953–11960.
15. Fancy, D.A., and Kodadek, T. (1998). A critical role for tyrosine residues in His6-Ni-mediated protein cross-linking. Biochem. Biophys. Res. Commun. *247*, 420–426.
16. Amini, F., Kodadek, T., and Brown, K.C. (2002). Protein affinity labeling mediated by genetically-encoded peptide tags. Angew. Chem. Int. Ed. Engl. *41*, 356–359.
17. Fancy, D.A., and Kodadek, T. (1999). Chemistry for the analysis of protein-protein interactions: rapid and efficient cross-linking triggered by long wavelength light. Proc. Natl. Acad. Sci. USA *96*, 6020–6024.
18. Fancy, D.A., Denison, C., Kim, K., Xie, Y., Holdeman, T., Amini, F., and Kodadek, T. (2000). Scope, limitations and mechanistic aspects of the photo-induced cross-linking of proteins by water-soluble metal complexes. Chem. Biol. *7*, 697–708.
19. Lumb, M.J., and Danpure, C.J. (2000). Functional synergism between the most common polymorphism in human alanine: glyoxylate aminotransferase and four of the most common disease-causing mutations. J. Biol. Chem. *275*, 36415–36422.
20. Ottersbach, K., and Graham, G.J. (2001). Aggregation-independent modulation of proteoglycan binding by neutralization of C-terminal acidic residues in the chemokine macrophage inflammatory protein 1 alpha. Biochem. J. *354*, 447–453.
21. Paoli, P., Giannoni, E., Pescitelli, R., Camici, G., Manao, G., and Ramponi, G. (2001). Hydrogen peroxide triggers the formation of a disulfide dimer of muscle acylphosphatase and modifies some functional properties of the enzyme. J. Biol. Chem. *276*, 41862–41869.
22. Shen, W.-J., Patel, S., Hong, R., and Kraemer, F.B. (2000). Hormone-sensitive lipase functions as an oligomer. Biochemistry *39*, 2392–2398.
23. Smirnova, E., Shurland, D.-L., Newman-Smith, E.D., Pishvaee, B., and van der Bliek, A.M. (1999). A model for dynamin self-assembly based on binding between three different protein domains. J. Biol. Chem. *274*, 14942–14947.
24. Wolf, J., Gerber, A.P., and Keller, W. (2002). tadA, an essential tRNA-specific adenosine deaminase from Escherichia coli. EMBO J. *21*, 3841–3851.
25. Bitan, G., Lomakin, A., and Teplow, D.B. (2001). Amyloid β-protein oligomerization. J. Biol. Chem. *276*, 35176–35184.
26. Bossu, F.P., and Margerum, D.W. (1977). Need to get it. Inorg. Chem. *16*, 1210–1214.
27. Bannister, C.E., Raycheba, J.M.T., and Margerum, D.W. (1982). Ni-GGH need to get it. Inorg. Chem. *21*, 1106–1109.
28. Melcher, K., and Johnston, S. (1995). GAL4 interacts with TBP and coactivators. Mol. Cell. Biol. *15*, 2839–2848.
29. Xie, Y., Denison, C., Yang, S.-H., Fancy, D.A., and Kodadek, T. (2000). Biochemical characterization of the TATA-binding protein-Gal4 activation domain complex. J. Biol. Chem. *275*, 31914–31920.
30. Coleman, R.A., Taggart, A.K.P., Benjamin, L.R., and Pugh, B.F. (1995). Dimerization of the TATA-binding protein. J. Biol. Chem. *270*, 13842–13849.
31. Coleman, R.A., and Pugh, B.F. (1995). A kinetic mechanism by which the TATA-binding protein achieves sequence specific DNA binding. J. Biol. Chem. *270*, 13850–13859.
32. Bertolaet, B.L., Clarke, D.J., Wolff, M., Watson, M.H., Henze, M., Divita, G., and Reed, S.I. (2001). UBA domains of DNA damage-inducible proteins interact with ubiquitin. Nat. Struct. Biol. *8*, 417–422.
33. Salmeron, J.M., Langdon, S.D., and Johnston, S.A. (1989). Interaction between transcriptional activator protein LAC9 and negative regulatory protein GAL80. Mol. Cell. Biol. *9*, 2950–2956.
34. Ding, W.V., and Johnston, S.A. (1997). The DNA-binding and activation domains of Gal4p are sufficient for conveying its regulatory signals. Mol. Cell. Biol. *17*, 2538–2549.
35. Melcher, K., and Xu, H.E. (2001). Gal80-Gal80 interaction on

adjacent Gal4p binding sites is required for complete GAL gene repression. EMBO J. *20*, 841–851.
36. Bitan, G., Kirkitadze, M.D., Lomakin, A., Vollers, S.S., Benedek, G.B., and Teplow, D.B. (2003). Amyloid beta-protein (Abeta) assembly: Abeta 40 and Abeta 42 oligomerize through distinct pathways. Proc. Natl. Acad. Sci. USA *100*, 330–335.
37. Han, Y., and Kodadek, T. (2000). Peptides selected to bind the Gal80 repressor are potent transcriptional activation domains in yeast. J. Biol. Chem. *275*, 14979–14984.
38. Schreiber, S.L. (2003). The small molecule approach to biology. Chem. & Eng. 1199 News *81*, 51–61.
39. Kodadek, T. (2002). Protein-detecting microarrays. Trends Biochem. Sci. *27*, 295–300.
40. Kodadek, T. (2001). Protein microarrays: prospects and problems. Chem. Biol. *8*, 105–115.
41. Zhu, W., Williams, R.S., and Kodadek, T. (2000). A Cdc6-binding peptide selected using a bacterial two-hybrid-like system is a cell cycle inhibitor. J. Biol. Chem. *275*, 32098–32105.
42. Kuruvilla, F.G., Shamji, A.F., Sternson, S.M., Hergenrother, P.J., and Schreiber, S.L. (2002). Dissecting glucose signaling with diversity-oriented synthesis and small-molecule microarrays. Nature *416*, 653–657.
43. Liu, B., Han, Y., Corey, D.R., and Kodadek, T. (2002). Towards synthetic transcription activators: recruitment of transcription factors to DNA by a PNA-peptide chimera. J. Am. Chem. Soc. *124*, 1838–1839.
44. Sun, L., Johnston, S.A., and Kodadek, T. (2002). Physical association of the APIS complex and general transcription factors. Biochem. Biophys. Res. Commun. *296*, 991–999.
45. Parks, T.D., Leuther, K.K., Howard, E.D., Johnston, S.A., and Dougherty, W.G. (1994). Release of proteins and peptides from fusion proteins using a recombinant plant virus proteinase. Anal. Biochem. *216*, 413–417.
46. Xie, Y., Sun, L., and Kodadek, T. (2000). TATA-binding protein and the Gal4 transactivator do not bind to promoters cooperatively. J. Biol. Chem. *275*, 40797–40803.
47. Schagger, H., and von Jagow, G. (1987). Tricine-sodium dodecyl sulfate-polyacrylamide gel electrophoresis for the separation of proteins in the range from 1 to 100 kDa. Anal. Biochem. *166*, 368–379.